Makromol. Chem., Macromol. Symp. 37, 53-66 (1990)

SPIN DYNAMICS IN CONDUCTING POLYMERS

Kenji Mizoguchi

Department of Physics, Tokyo Metropolitan University, Setagaya-ku, Tokyo, 158, Japan

Abstract: It is demonstrated that spin dynamics study is useful for what kinds of systems, on what theoretical basis of analysis, with what kinds of techniques and to get what kinds of information, showing a nice example of polyacetylene. Usefulness of electron spin resonance (ESR) study is stressed especially in a wide frequency range from 5 to 24000 MHz.

INTRODUCTION

In the recent 10 years polyacetylene as a prototype of conducting polymers has received a lot of interest not only from academic but also from practical view-point. Pristine trans-polyacetylene is a semiconductor with a conductivity of 10^{-6} S/cm and can be transformed by doping with an acceptor- (e.g. iodine, AsF_6^-, $FeCl_4^-$ etc.) or a donor- (e.g. alkaline metals) to "metal" with a conductivity up to nearly 10^5 S/cm (Ref. 1). To study this interesting system, we must face some difficulties; macroscopic techniques such as transport measurements would scarcely give information on the intrinsic behavior of the regular polymer crystals, because polymers, in general, have a structure of higher order than the basic crystal structure; e.g. a fibril structure in polyacetylene. To get knowledge by removing this difficulty, a spin dynamics study using magnetic resonance techniques such as NMR and ESR becomes a powerful tool, because they give microscopic information on the motion spectra of charged carriers through the motion of spins. This technique is useful for all the cases of regular crystals, disordered ones and amorphous ones.

In the case of polyacetylene, the spin-lattice relaxation rate of proton (^1H) nuclei has been measured as a function of frequency f on pristine and AsF_6^- doped polyacetylene by Nechtschein et al. in the early stage of investigation (Ref.2). They found that the relaxation rate is proportional to $1/\sqrt{f}$ on both pristine and doped polyacetylene, which coincides with a characteristic motion spectrum of one-dimensionally (1-D) diffusing spin. In pristine polyacetylene the presence of a neutral soliton, which is a spin carrying topological defect, as indicated in Fig.1, was a controversial point. They made a quantitative analysis of the on-chain diffusion rate of the neutral soliton to be more than 10^{13} rad/s. In the case of doped polyacetylene it was difficult to discriminate whether the spin carrying charged carrier or the residual neutral soliton dominates the proton relaxation rate. The experimental understanding of this problem is under way in our laboratory. On the dynamics of the neutral soliton, the presence of the neutral soliton and its dynamics

 CCC 0258-0322/90/$ 02.00

as a function of temperature with the relaxation rate and the Overhauser effect could be observed (Refs. 3-4).

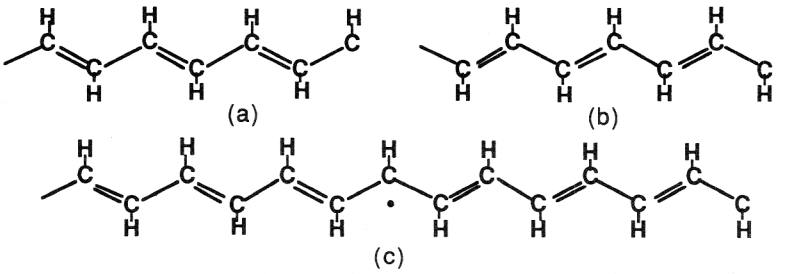

Fig. 1. trans-Polyacetylene : (a) and (b): two different phases of bond order, (c): neutral soliton as a domain wall of the two phases

NMR and ESR are complementary to each other. NMR relaxation rate observes indirectly the electron spin motion, and ESR does it more directly than NMR. This statement does not necessarily mean that NMR is inferior to ESR. Both techniques have some advantage and disadvantage. It is the best way to utilize both techniques to solve the spin dynamics correctly.

One of the disadvantage of NMR technique is the presence of a relaxation to a spatially fixed paramagnetic electron spin, which gives the same frequency spectrum of the spin-lattice relaxation rate as that ($\propto 1/\sqrt{f}$) for the electron spin diffusing along the 1-D chain (Ref.5). ESR technique compensates this disadvantage of NMR (Refs. 6-8), because the relaxation rate of ESR has no such process. A characteristic point of the NMR technique is that a theoretical expression of the relaxation rate includes two characteristic frequencies ; the Larmor frequency of nuclei, f_n, and that of electron spins, f_e, which effectively enlarge the frequency range which can be studied. In contrast with this, since ESR relaxation rate is only proportional to f_e and $2f_e$, the analysis will be simple. Finally it is noted that an anisotropic behavior is very helpful for understanding of the spin dynamics (Ref.9).

This paper presents in detail a review on a spin dynamics study, mainly by use of ESR technique.

THEORETICAL BACK GROUND OF SPIN DYNAMICS STUDY

Relaxation phenomena and spin motion

For simplicity we consider only an extreme narrowing case in which the characteristic time constant is much smaller than the Larmor period. Here, the characteristic time means a mean hopping time between available sites. If the system is anisotropic, the shortest one should hold this condition. The applicability of our

technique will be limited by this condition. Although this condition will be removed using a more complicated analysis, we will not treat further.

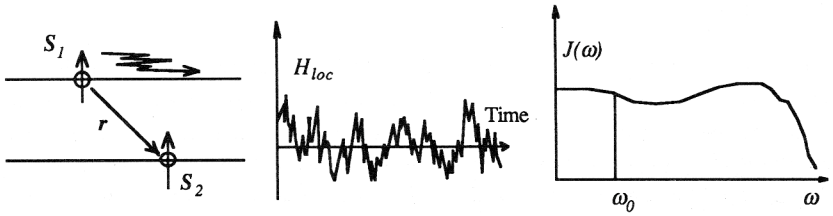

Fig. 2. Schematic explanation of the fluctuating local field (center) and the spectral density (right) produced by the diffusing spin S_2 at the spin S_1

At first we will consider the effect of the fluctuating magnetic fields on the magnetic relaxation phenomena (Fig.2). An electron spin which is rapidly diffusing (random walking in the same meaning) in a crystal produces dipolar and/or hyperfine fields fluctuating rapidly with time at the nucleus or the other electron spins (Fig.2, center). With an idea of the Fourier analysis an auto-correlation function $G(\tau)$ of this fluctuating field can be interpreted as a sum of various frequency components $J(\omega)$ from d.c to infinite, where ω is a angular frequency (Fig.2, right). What kind of effect of this magnetic fields on the nuclear or electron spins will be expected? The spins flip their direction absorbing a resonance (Larmor) frequency component of this fluctuating field in the same manner as the magnetic resonance. This flipping forces the spin system to equilibrate with the lattice temperature. After a characteristic time constant which is called the spin-lattice relaxation time T_1 the system reaches to the thermal equilibrium magnetization. Then, a measured T_1 should be proportional to the spectral density $J(\omega)$ of the auto-correlation function $G(\tau)$ of the fluctuating local field:

$$J(\omega) = \int_{-\infty}^{\infty} G(\tau)\, e^{-i\omega\tau}\, d\tau \qquad (1)$$

$$G(\tau) = \overline{H_{loc}(t)H_{loc}(t+\tau)} \qquad (2)$$

where the bar means an ensemble average. Therefore, by measuring T_1 as a function of frequency we can obtain a frequency dependence of the spectral density.

Following a definition of Abragam (Ref.10) the auto-correlation function $G(\tau)$ is expressed by

$$G(\tau) = \overline{F(t)F^*(t+\tau)}$$

$$= \int\int p(r_1,t)\, \Phi(r_1,r_2,\tau)\, F(r_1)F^*(r_2)\, dr_1 dr_2 \qquad (3)$$

$$= C_1 \sum_{r_1}^{n} \sum_{r_2}^{n} p(r_2,t)\ \Phi(r_1,r_2,\tau)\ F(r_1)F^*(r_2), \qquad (4)$$

where $F(t)$ is the random function of the time, $F(r)$ the random function of the distance r between two spins and also that of the time t implicitly, $p(r,t)$ the probability that the spin would be found in the distance r at t, which should be the spin concentration c and $\Phi(r_1,r_2,\tau)$ is the probability density that the spin which is known to be in r_1 at t would be found in the other distance r_2 after the time τ. For a discrete system the double integrals should be replaced by the double summations as shown in Eq.(4) where C_1 is the numerical parameter with a unit of length accompanying the lattice sum in discrete system. A functional form of the probability density $\Phi(r_1,r_2,\tau)$ is determined mainly by a manner of spin motion; dimensionality of the motion. On the other hand $F(r_1)F^*(r_2)$ depends on a type of interactions between spins; dipolar and scalar couplings.

Dimensionality and spectral density $\phi(\omega)$ of probability $\Phi(r_1,r_2,\tau)$

Dimensionality of the spin motion is reflected in the spectral density $\phi(\omega)$ which is defined as the Fourier transform of the probability function $\Phi(r_1,r_2,\tau)$:

$$\phi(\omega) = \int_{-\infty}^{\infty} \Phi(r_1,r_2,\tau) e^{-i\omega\tau} d\tau. \qquad (5)$$

One approach to discuss the spectral density is the diffusion equation:

$$\frac{\partial \Phi(r_1,r_2,\tau)}{\partial \tau} = \mathcal{D} \Delta \Phi, \qquad \mathcal{D}_i = D_i C_{1i}^2 \qquad (6)$$

where $\mathcal{D}_i$ is the diffusion coefficient (cm^2/s), D_i the diffusion rate (rad/s) and C_{1i} the coefficient (cm) comes from the discreteness of the real system. The suffix i indicates x, y and z. The solution of n-dimensional isotropic diffusion equation is given by well known formula,

$$\Phi(r_1,r_2,\tau)_{n\text{-}D} = \frac{1}{(\sqrt{4\pi D\tau})^n} \exp\{-\frac{((r_1-r_2)/C_1)^2}{4D\tau}\} \qquad (7)$$

For a quasi-one-dimensional (Q1D) case as polyacetylene one has the expression

$$\Phi(r_1,r_2,\tau)_{Q1D} = \frac{1}{\sqrt{4\pi D_{//}\tau}} \exp\{-\frac{((r_1-r_2)/C_{//})^2}{4D_{//}\tau}\} \exp(-D_\perp \tau) \qquad (8)$$

where $D_{//}$ and $C_{//}$ are the diffusion rate and the lattice constant along Q1D direction, respectively and $D_\perp$ is the diffusion rate perpendicular to the Q1D direction, which is introduced by taking into account the probability to escape from the Q1D path to the other (Ref.11).

The other approach is anisotropic random walk treatment (Ref.12). With the hopping rates D_1, D_2 and D_3 along the three directions one has a return probability to the same site as the original one after the time τ

$$\Phi(\tau) = e^{-2\tau(D_1+D_2+D_3)} [I_o(2D_1\tau)\cdot I_o(2D_2\tau)\cdot I_o(2D_3\tau)] \tag{9}$$

where $I_o(x)$ is the modified Bessel function and has limiting values as follows:

$$I_o(x) = \frac{1}{\pi}\int_0^{\pi} e^{x\cos\theta}\, d\theta \quad \rightarrow \quad \begin{cases} 1 & (x \to 0) \\ \dfrac{e^x}{\sqrt{2\pi x}} & (x \to \infty) \end{cases} \tag{10}$$

For the Q1D case, one gets the probability function as

$$\Phi(\tau)_{Q1D} = \frac{1}{\sqrt{4\pi D_1\tau}} e^{-2(D_2+D_3)\tau} \rightarrow \frac{1}{\sqrt{4\pi D_{//}\tau}} e^{-2D_\perp\tau}, \text{ at } D_{//}\tau >> 1 \tag{11}$$

where $D_\perp = D_2+D_3$, $D_{//} = D_1 >> D_2 \geq D_3$. This expression agrees with Eq.(8) except for the factor 2 in the argument of the exponential and the range function in Eq.(8).

Equations (5) and (11) yields the spectral density for the Q1D case as

$$\phi(\omega)_{Q1D} = \frac{1}{\sqrt{4D_{//}D_\perp}} \sqrt{\frac{1+\sqrt{1+(\omega/2D_\perp)^2}}{1+(\omega/2D_\perp)^2}} \tag{12}$$

$$= \frac{1}{\sqrt{2D_{//}\omega}}, \qquad \text{at the medium frequencies } D_\perp << \omega << D_{//} \tag{13}$$

$$= \frac{1}{\sqrt{2D_{//}D_\perp}}, \qquad \text{at the low frequencies } \omega << D_\perp \tag{14}$$

Since Eq.(11) does not include the range function in Eq.(8), these relations valid for the short-range scalar coupling or for the low frequency range $\omega << D_{//}/((r_1-r_2)/C_{//})^2$. Equation (8) gives the spectral density with more complicated formula,

$$\Phi(r_1,r_2,\tau)_{Q1D} = \phi(\omega)_{Q1D}\cdot\phi(|r_1-r_2|)_{Q1D} \tag{15}$$

and $\phi(|r_1-r_2|)_{Q1D} = e^{-\gamma u}\left[\cos(\gamma u) - \frac{v}{u}\sin(\gamma u)\right]$

where

$$\gamma = |r_1-r_2|\sqrt{\frac{2D_\perp}{D_{//}}}, \quad u = \sqrt{\frac{\sqrt{1+(\omega/2D_\perp)^2}+1}{2}}, \text{ and } \quad v = \sqrt{\frac{\sqrt{1+(\omega/2D_\perp)^2}-1}{2}}$$

At the much lower frequencies than $D_{//}/((r_1-r_2)/C_{//})^2$, $\phi(|r_1-r_2|)_{Q1D}$ approximately unity, that is, Eq.(12) is a good approximation even in the dipolar couplings. At the comparable frequency with $D_{//}/((r_1-r_2)/C_{//})^2$ one should, however, estimate the

spectral density of the auto-correlation function with the relation

$$J(\omega)_{Q1D} = c\, C_{//}\phi(\omega)_{Q1D} \sum_{r_1} \sum_{r_2} F(r_1)F^*(r_2)\bullet\phi(|r_1-r_2|)_{Q1D} \qquad (16)$$

An effect of $\phi(|r_1-r_2|)_{Q1D}$ will appear as a negative intercept of the vertical axis in $1/T_1$ versus $1/\sqrt{f}$ plot as typically shown in ^{1}H NMR $1/T_1$ of trans-polyacetylene at low temperatures (Ref.4).

T_1 , T_2 and interactions between spins

Interactions concerning the present problem are dipolar and scalar couplings between the electrons and between the electron and the nucleus. It is a important point that another interaction, independent of the spin motion (for example, coupling with phonons and spin orbit scattering by heavy nuclei) which can contribute to T_1 and T_2, should be enough small especially in ESR measurement, because very broad line width which is independent of the spin motion obscure analysis and signal at low frequency. Here, it should be noted that the dipolar interaction is a long range anisotropic coupling, but the scalar one is isotropic on site interaction in nature. Then, the scalar coupling is easier to treat than the dipolar one.

In general a hamiltonian can be expressed as

$$\mathcal{H}_I = \sum_q F_q\, A_q \qquad (17)$$

where A_q is the spin operator term and F_q is the range function. For the scalar coupling the hamiltonian is as follows (in this article, we determine that S is the electron spin and I is the nuclear and/or electron spin),

$$\mathcal{H}_I = F_S(t)\, \boldsymbol{I}\bullet\boldsymbol{S}, \qquad (18)$$

$$F_S = \delta(r_I - r_S), \qquad A_S = \frac{a}{2}\left(I_z S_z - \frac{I_+S_- + I_-S_+}{2}\right) \qquad (18a)$$

where a is the scalar coupling constant and the others are the usual spin operators. For the dipolar case, the formulae are given by

$$\mathcal{H}_I = \frac{\alpha}{r^3}\left\{\boldsymbol{I}\bullet\boldsymbol{S} - 3\frac{(\boldsymbol{I}\bullet\boldsymbol{r})(\boldsymbol{S}\bullet\boldsymbol{r})}{r^3}\right\}, \qquad (19)$$

$$F_o = \frac{1-3\cos^2\theta}{r^3}, \qquad A_o = \alpha\left\{I_z S_z - \frac{1}{4}(I_+S_- + I_-S_+)\right\} \qquad (19a)$$

$$F_1 = \frac{\sin\theta\cos\theta\, e^{\pm i\varphi}}{r^3}, \qquad A_1 = -\alpha\frac{3}{2}(I_z S_\pm + I_\pm S_z) \qquad (19b)$$

$$F_2 = \frac{\sin^2\theta\, e^{\pm 2i\varphi}}{r^3}, \qquad A_2 = -\alpha\frac{3}{4}(I_\pm S_\pm) \qquad (19c)$$

where $\alpha = \gamma_I\gamma_S\hbar$ and r, θ and φ are the polar co-ordinate of the vector between the spins S and I. It should be noted that the scalar interaction is isotropic, but the dipolar one is anisotropic. This anisotropy is useful for identification of relaxation

mechanisms (Ref.9). Equation(19a) is a diagonal term and Eqs.(19b) and (19c) are off-diagonal terms and have matrix elements for $|\Delta m|=1$ (absorption of $\hbar\omega_o$) and $|\Delta m|=2$ ($2\hbar\omega_o$) transition, respectively.

Following Abragam (Ref.10) with these formulae we have expressions of T_1 and T_2 for the scalar (isotropic hyperfine) couplings as,

$$T_{1S}^{-1}=c_I C_1 \frac{a^2}{3} I(I+1)\phi(\omega_S-\omega_I)\{1-\frac{S(S+1)(<Iz>-Io)}{I(I+1)(<Sz>-So)}\}, \tag{20}$$

$$T_{2S}^{-1}=c_I C_1 \frac{a^2}{3} I(I+1)\frac{1}{2}[\phi(0)+\phi(\omega_S-\omega_I)], \tag{21}$$

where $\phi(\omega)=\int_{-\infty}^{\infty}\Phi(r_1,r_2,\tau)e^{-i\omega\tau}d\tau$ is the spectral density of the probability function $\Phi(r_1,r_2,\tau)$ and c_I is the concentration of the spin I which is unity if each site has I spin as in usual ESR case. In this case Eq.(5a) predicts a mutual spin flip-flop between the I and S spins absorbing a difference energy of $\hbar(\omega_S-\omega_I)$. In Eq.(20) cross-relaxation (second) term can usually be neglected because of its small magnitude (see Ref.(10) for detail).

For the dipolar interaction between equal spins ($I=S$), that is, ESR case, T_1 and T_2 are written as follows;

$$T_{1S}^{-1}=\frac{2}{3}\alpha^2 S(S+1)[J_1(\omega_S)+J_2(2\omega_S)], \tag{22}$$

$$T_{2S}^{-1}=\frac{3}{8}\alpha^2 S(S+1)[J_0(0)+10J_1(\omega_S)+J_2(2\omega_S)], \tag{23}$$

and for polycrystalline samples by taking an ensemble average;

$$T_{1S}^{-1}=c_S C_1\alpha^2 S(S+1)\Sigma_1[0.2\phi(\omega_S)+0.8\phi(2\omega_S)], \tag{24}$$

$$T_{2S}^{-1}=c_S C_1\alpha^2 S(S+1)\Sigma_1[0.3\phi(0)+0.5\phi(\omega_S)+0.2\phi(2\omega_S)], \tag{25}$$

$$\Sigma_1=\sum_{r_1}^{n}\sum_{r_2}^{n}\frac{P_2(\cos\theta_{12})}{r_1^3\cdot r_2^3},$$

where Σ_1 is the powder averaged lattice sum $\sum\sum F(r_1)F^*(r_2)$ (Ref.13) and c_S is the concentration of the S spin. In the dipolar case the energy absorption of $2\omega_S$ appear, which corresponds to $|\Delta m|=2$ transition. It should be noted that $D_{//}$ have to be replaced by $2D_{//}$ in the case of mutual diffusion as in the present electron-electron dipolar coupling case.

Expressions for the dipolar interaction between unlike spins, that is the anisotropic hyperfine coupling, are somewhat complicated;

$$T_{1S}^{-1}=\frac{1}{12}\alpha^2 I(I+1)[J_0(\omega_S-\omega_I)+18J_1(\omega_S)+9J_2(\omega_S+\omega_I)]$$

$$+\frac{1}{12}\alpha^2 S(S+1)[-J_0(\omega_S-\omega_I)+9J_2(\omega_S+\omega_I)]\frac{<I_z>-I_0}{<S_z>-S_0}, \quad (26)$$

$$T_{2S}^{-1}=\frac{1}{24}\alpha^2 I(I+1)[4J_0(0)+J_0(\omega_S-\omega_I)+18J_1(\omega_I)+36J_1(\omega_S)+9J_2(\omega_S+\omega_I)], \quad (27)$$

and taking the average for the powder crystalline sample, we get

$$T_{1S}^{-1}=\frac{2}{3}c_I\, C_1\alpha^2 I(I+1)\Sigma_1[0.1\phi(\omega_S-\omega_I)+0.3\phi(\omega_S)+0.6\phi(\omega_S+\omega_I)]$$
$$+\frac{2}{3}c_I\, C_1\alpha^2 S(S+1)\Sigma_1[-0.1\phi(\omega_S-\omega_I)+0.6\phi(\omega_S+\omega_I)]\frac{<I_z>-I_0}{<S_z>-S_0}, \quad (28)$$

$$T_{2S}^{-1}=\frac{1}{3}c_I\, C_1\alpha^2 I(I+1)\Sigma_1[0.4\phi(0)+0.1\phi(\omega_S-\omega_I)+0.3\phi(\omega_I)+0.6\phi(\omega_S)+0.6\phi(\omega_S+\omega_I)], \quad (29)$$

and if one applies a condition $\omega_S >> \omega_I$ which valids for ESR,

$$T_{1S}^{-1}\cong\frac{2}{3}c_I\, C_1\alpha^2 I(I+1)\Sigma_1\phi(\omega_S)\{1+\frac{1}{2}\frac{S(S+1)<I_z>-I_0}{I(I+1)<S_z>-S_0}\}, \quad (30)$$

$$T_{2S}^{-1}\cong\frac{1}{3}c_I\, C_1\alpha^2 I(I+1)\Sigma_1[0.4\phi(0)+0.3\phi(\omega_I)+1.3\phi(\omega_S)]. \quad (31)$$

For NMR case, by exchanging I and S in Eqs.(28) and (29) one has

$$T_{1I}^{-1}\cong\frac{2}{3}c_S\, C_1\alpha^2 S(S+1)\Sigma_1\{[0.3\phi(\omega_I)+0.7\phi(\omega_S)]+0.5\phi(\omega_S)\frac{I(I+1)<S_z>-S_0}{S(S+1)<I_z>-I_0}\}, \quad (32)$$

$$T_{2I}^{-1}\cong\frac{1}{3}c_S\, C_1\alpha^2 S(S+1)\Sigma_1[0.4\phi(0)+0.6\phi(\omega_I)+\phi(\omega_S)]. \quad (33)$$

Here, Σ_1 should be estimated for each cases mentioned above. The second terms of $1/T_1$ in Eqs.(20,26,28,30,32) are contribution from the cross-relaxation between I and S spins and are origin of the Overhauser enhancement effect (Ref.10). In the present extreme narrowing case one peculiar relation $1/T_1 = 1/T_2$ is easily found under the low frequency limit in Eqs.(24) and (25). In all the cases mentioned above this relation approximately hold. $1/T_1$ always function of the frequency, but $1/T_2$ includes the frequency independent term $\phi(0)$ which is called as a secular broadening $1/T_2'$. The frequency dependent terms are so-called life time or non-secular broadening $1/T_1'$ which origin is the same as $1/T_1$. The ratio of $1/T_1'$ to $1/T_1$ is 7/10 for the dipolar coupling between electrons (Eq.(25)), 8/10 for the anisotropic hyperfine coupling (Eqs.(31) and (33)) and 5/10 for the isotropic hyperfine coupling (Eq.(33)). These values are useful to discriminate these relaxation mechanisms.

EXPERIMENTAL

How to observe ESR down to 5 MHz

The characteristic feature of the present experiment is to measure the relaxation rates over the wide frequency range from several to several tenth thousand MHz. The frequency of the conventional ESR equipment is 9-10 GHz, the so-called X-band,

in which the wave length is nearly 3 cm. Then, a resonant cavity is utilized. In the present case, especially less than 1000 MHz, its wave length is long enough to use a conventional resonant circuit with coil and capacitor. In Table I sensitivities of both ^1H NMR and ESR in trans-polyacetylene at the same frequency are compared with each other. Although the integrated intensity of NMR is higher than that of ESR by a factor of 4, the peak intensity of ESR is much higher than that of NMR. This relation depends on the spin concentration and the line width in the samples. For studies at low frequency the line width should be narrow.

Table I. Comparison of the sensitivity between NMR and ESR at the same frequency in the case of trans-polyacetylene

	^1H NMR	ESR
Magnetization $M=\chi H_0 \propto \gamma^2 H_0 = \gamma\omega$	1	660
Spin concentration c	1	4×10^{-4}
Integrated intensity	1	0.27
ΔH_{pp} (Oe)	8	<1
Peak intensity	1/8~0.12	0.27

Pulse or continuous wave (CW) ?

The most conventional technique to measure the relaxation rates is the pulse technique, especially in NMR. The recent progress in ESR spectroscopy permits also the use of the pulse technique at the X-band. It is, however, very difficult to utilize the pulse technique in a wide frequency range in ESR, because of the short relaxation rate, less than 1 μs in ESR, and the longer dead time, more than several μs, at low frequencies intrinsically. The theoretical minimum recovery time constant is dominated by a ring down time constant δt of the resonator which can be characterized by the frequency and quality (Q-) factor as $\delta t \sim L/r \sim Q/\omega$. Typical values are 2 μs at 10 MHz (< 0.2 μs), 0.3 μs at 100 MHz (< 0.5 μs) and 0.1 μs at the X-band (several μs). The parentheses indicate the order of the relaxation time in trans-polyacetylene. A practical dead time of the pulse spectrometers would be several times longer than δt. Then, the practical technique at low frequency is the CW method.

Spectrometer

A home-made hybrid junction type spectrometer was used at less than 500 MHz (usable up to 2 GHz), with a high stability oscillator as a signal source. A homodyne with a double balanced mixer and phase shifted reference were used for detection. Two non-magnetic tuning air capacitors were equipped in vicinity of the samples. The detected signals were fed into a lock-in amplifier and digital signal analyzer with a magnetic field modulation and swept at a fixed frequency. A block diagram is

shown in Fig. 3.

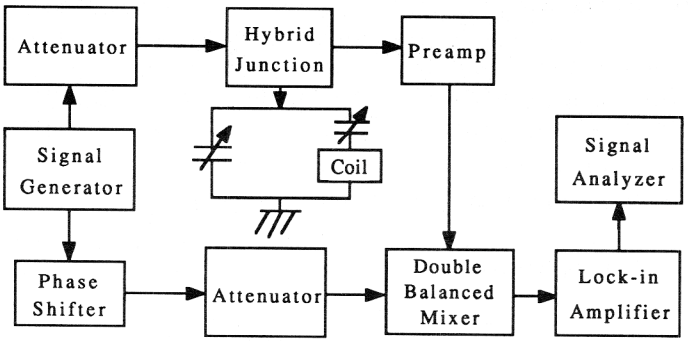

Fig. 3 Block diagram of the hybrid spectrometer. Samples are located in the coil and magnet

Measurements of relaxation rate

The ESR line shape of the electron spin which diffuses very rapidly should give the Lorentzian line shape. In this case the Bloch phenomenological equation should hold, and the absorption signal of ESR can be expressed by

$$\chi'' = \chi_0 \frac{H_1 \gamma T_2^*}{1+\gamma^2 H_1^2 T_1 T_2^* + ((H-H_0)\gamma T_2^*)^2}, \qquad \Delta H_{1/2} = \frac{1}{\gamma T_2^*}. \tag{34}$$

One can get the spin-lattice relaxation rate to measure signal intensities as a function of magnitude of the radio frequency field H_1. Here T_2^* can be estimated from the ESR line width, and calibration of H_1 was achieved with use of several reference samples in which the origin of the line width is ascribed to the life time broadening and the relation $1/T_1 = 1/T_2$ should hold. The reference samples are listed in Table II.

Table II. Reference samples for H_1 calibration

Samples	Stability	line width
(Tri-p-nitrophenyl)methyl radical	unstable in air	$\Delta H \sim 0.4$ Oe
Qn(TCNQ)$_2$	stable	$\Delta H \sim 0.168$ Oe
Ad(TCNQ)$_2$	stable	$\Delta H \sim 0.136$ Oe

The transverse relaxation rate can be obtained from the frequency dependence of the line width. In the determination of the line width the next three points should be noted : saturation of signals, over-modulation and magnetic field inhomogeneity

and stability.

TYPICAL RESULT AND INTERPRETATION IN TRANS-POLYACETYLENE

Spin-concentration dependence of $1/T_1$ (Ref.6)

Figure 4 which indicates $1/T_1$ as a function of the neutral soliton concentration c, clearly demonstrates an identification of the relaxation mechanism. A peculiar feature of this Figure is that the relaxation rates can be separated into two contributions: one being proportional to the spin concentration c and the the other the frequency independent positive intercept on the $1/T_1$ axis. The former may be ascribed to the electron-electron dipolar coupling which is a unique candidate proportional to the spin concentration in ESR. The latter may be interpreted to be the hyperfine coupling with ^1H or ^2D nuclei in origin. As expected, the magnitude of the constant term for t-(CH)x is larger than that for t-(CD)x by the ratio $(\gamma_H I_H(I_H+1)/\gamma_D I_D(I_D+1))^2 \sim 16$. Since in both systems the proportional coefficients show a similar magnitude, it is supposed that the diffusion rates are similar to each other. From these data the relaxation mechanism in t-polyacetylene was clearly identified.

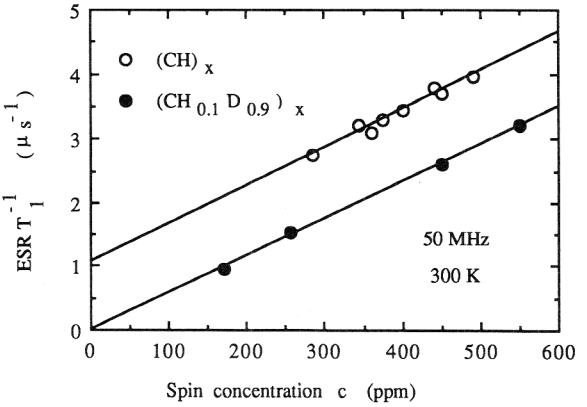

Figure 4 . Concentration dependence of ESR T_1

Frequency dependence of $1/T_1$ (Ref.6)

Figure 5 shows the frequency variation of $1/T_1$ in the wide frequency range (Ref.6). Along the identified mechanisms the data was analyzed to deduce many information, which prediction is shown to agree very well with the data by the solid curves in this figure. These data say how the neutral soliton diffuse in the crystal; $\approx 10^{13}$ rad/s on-chain and $\approx 10^8$ rad/s interchain hopping rates. These values agree well with the conclusion drawn by Nechtschein et al. from ^1H NMR (Ref.4). Therefore, the presence of the neutral soliton in trans-polyacetylene was strongly confirmed. Unfortunately, however, it would be difficult to measure $1/T_1$ down to

less than 100 K, because it is known that the ESR signal becomes inhomogeneous at lower temperatures due to the presence of a so-called neutral soliton trapping effect (Ref.4, 6-9). To overcome this difficulty the line width $1/T_2$ was analyzed in detail.

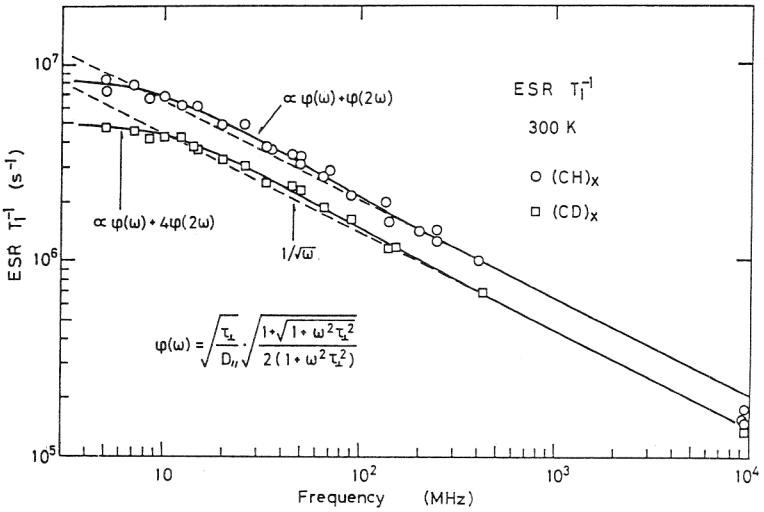

Fig. 5 Frequency dependence of ESR $1/T_1$ in t-(CH)x and t-(CD)x.

Temperature variation of the ESR line width (Refs. 7,8)

The temperature variation of the ESR line width in t-(CH)x is shown as a function of $1/\sqrt{f}$ in Fig.6. Normal quasi-1-D behavior, shown by the solid curves at high frequency, and the anomalous broadening shown by the broken lines at low frequency (right hand side of this figure), are the characteristic feature of this data. To increase the accuracy, ESR line shapes were fitted to the Lorentzian by the least square method. Analysis of the data at higher frequencies yields the temperature dependence of the on-chain hopping rate $D_{//}$, as shown in Fig. 7, and the inter-chain hopping rate $D_\perp$. The T^2 temperature variation of $D_{//}$, as easily found in Fig. 7, was of theoretical interest (Refs. 14,15).

The abnormal broadening at low frequency can be successfully interpreted by the appearance of the non-secular (off-diagonal) broadening with decreasing the Larmor frequency down to the frequency of an effective anisotropic hyperfine coupling. It has been suggested that the neutral soliton should be delocalised over 15 carbon sites (Refs.16,17). From the analysis of this anomaly one can estimate the maximum spin density of the delocalised spin distribution as $\rho \approx 0.14$-0.18 (Ref.8).

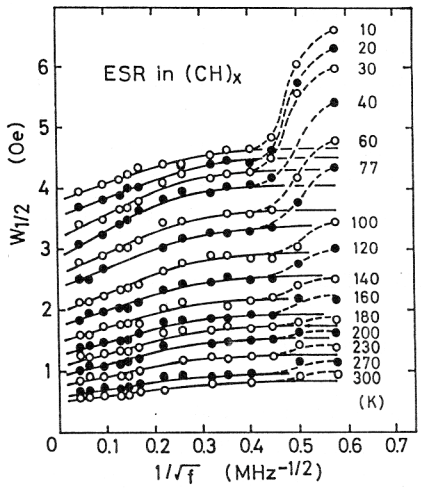

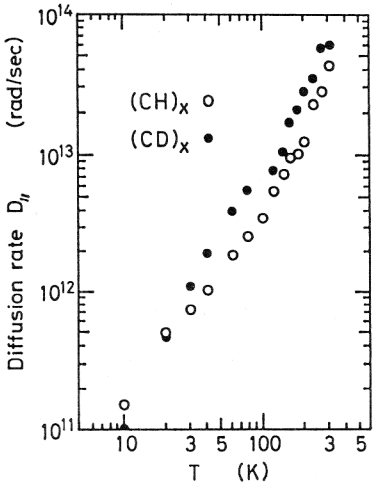

Fig. 6 (left) The frequency variation of the ESR line width in t-(CH)x.
Fig. 7 (right) The temperature dependence of the on-chain diffusion rate.

PERSPECTIVE

The main purpose of the described technique is to investigate the dynamics of charged and spin carrier in conducting materials from a microscopic view point. With this intention we proceed experiments and analyses on a heavily doped polyacetylene and a protonated polyaniline. For the latter system we have already found some interesting behaviors and reported in this summer school (Refs.18,19). Since this technique is not extensive to all materials, it is important to select useful systems to be studied.

ACKNOWLEDGEMENT

This work was supported in part by the Yamada Science Foundation.

REFERENCES

(1) For example, see the proceedings of ICSM'88 (Santa Fe), Synth.Metals **27**, (1988) - **28** (1989)

(2) M. Nechtschein, F. Devreux, R.L. Greene, T.C. Clarke and G.B. Street, Phys.Rev.Lett. **44**, 356 (1980)

(3) K. Holczer, J.P. Boucher, F. Devreux and M. Nechtschein, Phys.Rev. B **23**, 1051 (1981),

(4) M. Nechtschein, F. Devreux, F. Genoud, M. Gugilelmi and K. Holczer, Phys.Rev. B **27**, 61 (1983)

(5) N.S. Shiren, Y. Tomkiewicz, T.G. Kazayaka and A.R. Taranko, Solid St. Commun. **44**, 1157 (1982)

(6) K. Mizoguchi, K. Kume and H. Shirakawa, Solid St. Commun. **50**, 213 (1984)

(7) K. Mizoguchi, K. Kume and H. Shirakawa, Synth. Metals **17**, 405 (1987)

(8) K. Mizoguchi, S. Komukai, T. Tsukamoto, K. Kume, M. Suezaki, K. Akagi and H. Shirakawa, Synth. Metals **28**, D393 (1989)

(9) K. Mizoguchi, K. Kume and H. Shirakawa, Solid St. Commun. **59**, 465 (1986)

(10) A. Abragam, Principles of Nuclear Magnetism, chapter 8, (Oxford, 1961)

(11) G. Soda, D.Jerome, M. Weger, J. Alizon, J. Gallice, H. Robert, J.M. Fabre and L. Giral, J. Phys. (Paris), **38**, 931 (1979)

(12) M.A. Butler, L.R. Walker and Z.G. Soos, J. Chem. Phys., **64**, 3592 (1976)

(13) C.A. Sholl, J. Phys. C **14**, 447 (1981) and references therein

(14) M. Ogata, A. Terai and Y. Wada, J. Phys. Soc. Jpn. **55**, 2305 (1986)

(15) S. Jeyadev and E.M. Conwell, Phys. Rev. Lett., **58**, 258 (1987)

(16) K.R. Subbaswamy and M. Grabowski, Phys. Rev. B, **24**, 2168 (1981)

(17) S. Kuroda, H. Bando and H. Shirakawa, J. Phys. Soc. Jpn, **54**, 3956 (1985)

(18) K. Mizoguchi, M. Nechtschein, J.P. Travers and C. Menardo, Synth. Metals, **29**, E417 (1989)

(19) K. Mizoguchi, M. Nechtschein, J.P. Travers and C. Menardo, Phys. Rev. Lett., **63**, 66 (1989)